

INFLUENCE OF CERAMIC WASTE AND CEMENT ON THE MECHANICAL AND HYDRAULIC PROPERTIES, AND MICROSTRUCTURE OF THE ROAD SUB-BASE LAYER

SADEK DEBOUCHA^{1,2}, HOCINE ZIANI¹, ABDERRACHID
AMRIOU³, WALID MAHERZI⁴, WALID DEBOUCHA⁵

¹*Department of Civil Engineering, University Mohamed El Bachir El Ibrahim
of Bordj Bou Arreridj, El Annasser, 34000, Algeria*

²*Laboratory of Structure Intelligent, University of Ain T'emouchent, Algeria*

³*Department of Civil Engineering, University Mohamed Boudiaf M'sila, 28000,
Algeria*

⁴*Laboratoire de Génie Civil et Géo-Environnement, University of Lille, Lille,
France*

⁵*LMGC, University Montpellier, CNRS, Montpellier, France*

Received 11 March 2024; accepted 30 July 2024

* Corresponding author. E-mail: s.deboucha@univ-bba.dz

Sadek DEBOUCHA (ORCID ID 0000-0002-0023-1293)

Hocine ZIANI (ORCID ID 0009-0001-8851-1993)

Abderrachid AMRIOU (ORCID ID 0000-0002-4933-3477)

Walid Maherzi (ORCID ID 0000-0002-8957-2974)

Walid Deboucha (ORCID ID 0000-0003-4798-8741)

Copyright © 2024 The Author(s). Published by RTU Press

This is an Open Access article distributed under the terms of the Creative Commons Attribution License (<http://creativecommons.org/licenses/by/4.0/>), which permits unrestricted use, distribution, and reproduction in any medium, provided the original author and source are credited.

Abstract. This study examines cement and ceramic waste (CW) for the sub-base layer of roads. This innovative method can do away with the risks associated with improper disposal of industrial waste. To achieve this objective, several proportions of cement and CW were used, ranging from 1.5 to 2% and 5% to 15%, respectively. The aim of the work was to examine the influences of CW and ordinary Portland cement (OPC) on the unconfined compressive strength (UCS), permeability, consolidation, and microstructures of untreated and treated soil of road sub-base layer. The Guelph permeameter, UCS, permeability, and one-dimensional consolidation were among the laboratory and in-situ tests that were examined; the microstructures were characterised using SEM, infrared (IR), and mercury intrusion porosimetry (MIP). The findings indicated that the high permeability of the natural soil caused harm to our road soon after construction. Applying 5 to 15% CW reduced permeability by approximately 100% and settlement by around 43%. Furthermore, under wet and immersed conditions, mixing CW and OPC with soil raised UCS by approximately 182% and 20 times, respectively. This study demonstrated that by enhancing the geotechnical properties of soil, CW and OPC combined with it could be used as a road sub-base layer material.

Keywords: amelioration, ceramic waste, mechanical-hydraulic properties, microstructure, OPC, road layers.

Introduction

Algeria produces thousands of tons of ceramic waste (CW) annually from the construction of thousands of new homes. According to Deboucha et al. (2020), using recycled materials is crucial to protecting natural resources. Road aggregate base and sub-base layers have been effectively constructed from recycled construction materials (Alurajah et al., 2012; Fransisco et al., 2012; Gautam et al., 2018). The key to getting rid of this waste is to use industrial waste materials to make substitute materials (Ahmed & Abouzeid, 2009). Most roads have a limited lifespan due to changing moisture conditions in road layers, particularly in our research area where heavy winter rains occur frequently. These changes cause a significant volume change in a short amount of time. Semi-rigid materials have been utilised for pavement for decades in many countries because they are very resistant to the impacts of climate change and have beneficial effects on strength, loading distribution, workability, and layer thickness reduction (Gnanendran & Dalim, 2016; Xuan et al., 2016).

Reusing CW to enhance soil properties has been the subject of numerous studies. According to Daniyal & Shakeel (2015), 54% of all building waste was made up of CW. Due to its high silica, aluminium, iron oxide, and calcium oxide content, ceramics are a good choice for improving layers of road concrete (Valdés et al., 2010). By reducing permeability, compressibility, and boosting strength, fine additions to

the soil improve the engineering qualities of various soil types for use in road layers (Ojuri & Opeyemi, 2014). When lateritic soil was stabilised with CW ranging from 0% to 30%, Olumuyiwa et al. (2019) saw a notable improvement in the geotechnical parameters. Addition of up to 40% CW in the construction sector resulted in reducing the pressure of swelling and potential swelling by about 86% and 57%, respectively (Koyuncu et al., 2004). Rajamannan et al. (2013) investigated the addition of CW to the clay materials and ceramic bricks as filler, thus promoting the safe and sustainable method of its reuse. Using coarse CW as an alternative material in highway construction can extend its life and limit the consumption of industrial spaces (Electricwala et al., 2013). Jafari & Esna-asari (2012) reported that the UCS increased by about 286% when they reinforced the clayey soil with waste. Reusing industrial waste to improve sub-base materials for road is the main focus of the current research. Algerian road sub-base materials have a high permeability and compressibility, which reduced their longevity and gave most roads a poor bearing capacity. The objective of this investigation is to assess the soil-beneficial effects of CW and ordinary Portland cement (OPC) and enhance the properties of the road sub-base layer. In order to recycle CW and lessen its negative effects on the environment, we looked into the possibility of combining CW and OPC with soil in the road sub-base layer. The specific goal of this effort was to make stabilised materials stronger while decreasing their permeability and compressibility.

1. Experimental program

1.1. Materials

1.1.1. Soil

The actual road project at Tixtar, Bordj Bou Arreridj, Algeria, as presented in Figure 1(a), which was undergoing repair, provided the natural soil. On natural soils, a mechanical and physical test was performed to measure permeability and unconfined compressive strength. Table 1 lists the fundamental properties of natural soil. The results show that the soaked CBR was 5% and the unsoaked CBR was 51%, respectively. This confirms that natural soil becomes troublesome when it is exposed to water because the bearing capacity of the soil drops significantly. Resilient modulus (Mr) values, however, varied from 54 to 65 MPa, which is significantly less than what the sub-base layer required. Furthermore, the Mr of stabilised soils varied from 77 to 596 MPa according to earlier research by Deboucha et al., (2020).

Table 1. Basic properties of natural soils

Properties	Values
Liquid limit, W_L , %	30.37
Plastic limit, W_p , %	24.05
Plasticity index, I_p , %	6.32
Dry density, γ_d , kN/m ³	19.4
The uniformity coefficient C_u , %	13.07
The coefficient of curvature C_c , %	1.44
Void ratio, e_0	0.095
Compacted soil cohesion C' , bar	1.58
Friction angle φ' , °	8.73

1.1.2. Ceramic waste

CW is classified as a non-recycled material in Algeria, the ceramic waste of flooring tile used in our work was collected from a recent building under construction, as presented in Figure 1(b), which uses this waste as coarse materials. The size ranged from 0 to 5 mm. The need to repurpose this waste in order to improve the properties of road layers as sub-base layers stems from the environmental impact and the

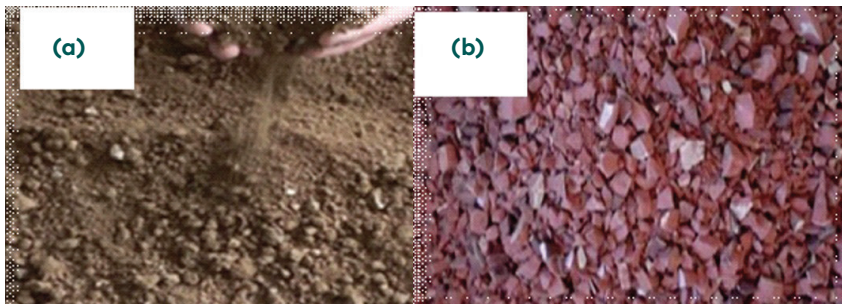


Figure 1. (a) Natural soil; (b) Ceramic waste

Table 2. Chemical composition of materials in %

Element	SiO ₂	AlO ₃	FeO ₃	CaO	MgO	SO ₃	K ₂ O	Na ₂ O	Li
Soil	25.35	15.53	4.54	35.64	4.38	3.54	3.63	2.62	4.77
CW	65.35	19.13	3.49	4.69	3.67	0.15	3.38	0.15	–
OPC	19.51	3.95	2.93	62.82	1.53	1.22	0.69	1.1	7.3

costs associated with road construction. In this study, the proportions of coarse material in the soil were 5%, 10%, and 15%. The chemical makeup of soil, CW, and OPC is shown in Table 2.

1.1.3. Ordinary Portland cement

In this project, Lafarge OPC (Matine Type II, 42.5 MPa) was utilised. In our research, OPC, which is often utilised to bind soil particles, was also found to be able to bind soil-CW particles. The chemical and physical characteristics of OPC are shown in Table 3.

Table 3. Physical properties and chemical composition of OPC

Designation	CEM-II/B 42.5 N NA 442 MATINE	
Physical properties	Normal consistency of the cement paste	25–28.5
	Blaine fineness	4160–5270 $\mu\text{m}/\text{m}$
	Initial setting	135–190 min
	End setting	190–285 min
	Shrink at 28 days	< 1000 $\mu\text{m}/\text{m}$
	Expansion	0.25–2.55 mm
	Compressive strength at 28 days	≥ 42.5 MPa
Chemical composition	Loss on ignition	7–12.5%
	Soluble residues	0.7–2%
	Sulfates	2–2.7%
	Magnesium oxide	1–2.2%
	Chlorides	0.01–0.05%
	Tricalcic silicates	55–62%
	Alkalis	0.5–0.75%

1.2. Methods

After the soil fundamental analysis was determined as presented in Table 1, it was air-dried at 105 °C and then run through a 5 mm sieve. Then, CW-OPC and CW alone were combined with the soil. As shown in Table 4, ratios of OPC were selected at 1.5% and 2% by total soil weight, whereas 5% to 15% of CW was selected based on weight. Based on the maximum dry density (MDD) and optimum moisture content (OMC), which are found via the modified proctor compaction test as presented in Table 5, each sample was combined for the various tests. In order to achieve the aim of the research, the Guelph permeameter in-situ test was used to determine the natural soil hydraulic conductivity in accordance with ASTM D 5126 (2016). The findings were analysed using the two-head approach, and constant pressure was applied inside a borehole to

measure the natural soil hydraulic conductivity. The sub-base layer that was built on the site to regulate the permeability of the soil served as the fixed GP. Figure 2 presents the Guelph permeameter.

Samples of natural soil, soil-CW, and soil-CW-OPC were subjected to the permeability test as presented in Figure 4 in this investigation.

Table 4. Mix design composition

Mix Design	Mixture composition	Mix Design	Mixture composition
S0	Natural soil	S6	Soil + 15% CW +1.5% C
S1	Soil +5% CW	S7	Soil +5% CW + 2%
S2	Soil + 10% CW	S8	Soil +10% CW +2% C
S3	Soil + 15% CW	S9	Soil +15% CW + 2% C
S4	Soil + 5% CW + 1.5% C	S10	Soil + 1.5% C
S5	Soil + 10% CW + 1.5% C	S11	Soil + 2% C

Note. C: Cement

Table 5. MDD and OMC of different mix design

Mix Design	MDD, g/cm ³	OMC, %	Mix Design	MDD, g/cm ³	OMC, %
S0	1.93	13.10	S6	1.93	12.50
S1	1.94	11.20	S7	1.97	11.32
S2	1.98	09.96	S8	1.95	11.42
S3	1.94	11.37	S9	1.95	11.80
S4	1.93	11.78	S10	1.95	12.25
S5	1.96	12.44	S11	1.95	12.20



Figure 2. Apparatus of Guelph permeameter



Figure 3. UCS hydraulic press and extruder of samples



Following a 24-hour storage period in plastic bags and a 28-day curing period in water at a fixed temperature of 20 ± 2 °C, the OPC specimens were compressed into three layers in a permeability mould using 25 blows for each layer. In addition, the specimens without cement were compressed in a permeability mould, kept for 24 h in plastic bags, and subsequently put through a falling-head permeability test in accordance with ASTM 5084-10 (2010).

The execution of CW and OPC in ameliorating the soil strength at optimum moisture contents (OMC) and density was carried out by the modified proctor compaction test, which prepared specimens for UCS by using static compaction of all mixtures.

For each mixture, we used the identical approaches to manage the energy and water of compaction. Following mixing, the raw ingredients listed in Table 6 were put into a 70 mm by 140 mm mould using the static compaction device shown in Figure 3. The specimens were then extruded from the mould and stored for a day in a plastic bag. The OPC specimens were immersed in water for 7, 14, and 28 days after being moved to the water tank. Furthermore, after being moved to a temperature-controlled chamber, the specimens with OPC for unsoaked circumstances healed for 7, 14, and 28 days. Additionally, the specimens without cement were kept in the plastic bags for a day before taking the reading. The UCS test was conducted using ASTM 2166-06 (2006) guidelines.

In order to evaluate the effect of CW on soil settlement behaviour, a number of consolidations were conducted in this work. In this set of experiments, natural soil was combined with 5%, 10%, and 15% of CW under dry conditions. OMC was then compacted in a mould at MDD.



Figure 4. Apparatus of permeability **Figure 5.** Apparatus of consolidation

Compressibility properties are often measured under the assumption of incremental loading (100, 200, 400, and 800 KPa). The test was carried out in compliance with ASTM D2435 (2011) as presented in Figure 5.

To forecast the microstructure of the samples, SEM and point elemental energy-dispersive X-ray (EDX) studies are also performed. Using an infrared spectrum and a Perkin Elmer Spectrum 2000 instrument, 200 mg of KBr and roughly 2 mg of dry mixes were blended-subjected to an infrared spectrum, and then scanned in order to determine changes in the microstructure of stabilised soil samples. To understand the themes of the treated and untreated soil at the microscopic level, MIP tests were investigated. We cut out a little cub that had sides that measured around 7 mm. We submerged it in nitrogen liquid and performed freeze-drying in the Alpha 1-4 LD for a day. We employed a Quantachrome porosimeter (AutoPore IV 9500 V1.09) to examine the pore size distribution of mixtures.

Table 6. Mix design of the treated soil for various laboratory tests

Set of test	Type of test	Purpose	Curing duration	Curing condition	Mix design
01	Guelph Permeameter	To determine the hydraulic conductivity of natural soil (field test)	–	–	In-situ
02	Permeability test (Falling head method)	To evaluate the rate of permeability of the test samples	28	Cure in water	S0, S1, S2, S3 S7 S8
03	Unconfined compression	To investigate the effect of CW and OPC on the UCS of the test specimens To investigate the effect of CW and OPC on the UCS of the test specimens	7, 14, 28	Wet and dry	S0, S1, S2, S3 S4, S5, S6, S7, S8, S9, S10, S11
04	Consolidation	To investigate the effect of CW and OPC on void ration and compressibility index	–	–	S0, S1, S2, S3
05	Infrared	Analysis microscopic	–	–	S0, S1, S2, S3, S4
06	Mercury intrusion prosimetry	Analysis microscopic	–	–	S0, S1, S2, S3, S4
07	SEM-EDS	Analysis microscopic	0, 28	–	S0, S7, S8, S9
08	FRX	Analysis microscopic	–	–	Soil, CW, OPC

2. Results and discussion

2.1. Guelph permeameter test (GP)

Reynolds & Elrick (1986) measured the field saturated hydraulic conductivity (K_{fs}) using GP by determining the steady-state liquid recharge rate (Q), which maintains a constant depth of water in the cylindrical auger hole in the unsaturated area. In this study, the calculation of K_{fs} used (Zhang et al., 1998) formulas. Based on the field GP testing, we summarised the results in Table 7. From Table 7, the hydraulic conductivity of natural soil is $K_{fs} = 2.13 \times 10^5$ cm/sec. These findings allow us to categorise our soil according to Darcy's classification system: silty sands or fine sands.

Table 7. Hydraulic conductivity (K_{fs})

Factor	Formula
Rate of flow for H_1	$Q_1 = Y \times R_1 = 3.24$ ($R_1=1.5$: Steady state rate of water level change cm/min)
Rate of flow for H_2	$Q_2 = Y \times R_2 = 4.32$ ($R_1 = 2$: Steady state rate of water level change cm/min)
Shape factor for H_1	$G_1 = \frac{H_2 C_1}{\pi(2H_1 H_2 (H_2 - H_1) + a^2 (H_1 C_2 - H_2 C_1))} = 0.005$
Shape factor for H_2	$G_2 = \frac{H_1 C_2}{\pi(2H_1 H_2 (H_2 - H_1) + a^2 (H_1 C_2 - H_2 C_1))} = 0.004$
Factors corresponding H_1/a	$C_1 = \left(\frac{\frac{H_1}{a}}{2.074 + 0.093 \left(\frac{H_1}{a} \right)} \right)^{0.754} = 0.809$
Factors corresponding H_2/a	$C_2 = \left(\frac{\frac{H_2}{a}}{2.074 + 0.093 \left(\frac{H_2}{a} \right)} \right)^{0.754} = 1.287$
Hydraulic conductivity	$K_{fs} = G_2 Q_2, G_1 Q_1 = 1.28 \times 10^3$ cm/min = 2.13×10^5 cm/s Soil classification: Silty sands or fine sands Classification of Darcy permeability 10^{-2} to 1 (high permeability)

2.2. Falling head permeability test

The coefficient of permeability k for both treated and untreated soil was investigated in a laboratory setting as presented in Figure 6, following the theory of Darcy (1856). The permeability was related to the dynamic water viscosity, which changes with temperature, but it was not persistent for the given soil parameters. Investigations were conducted on compacted samples of natural soil (S0), 5–15% CW-soil (S1, S2, and S3), and 5–10% CW-soil-OPC (S7, S8).

Figure 6 makes it evident that the permeability coefficient of the stabilised soil mixes is reduced by approximately 88% to 93% due to the action of CW and OPC. The percentage of CW added varied from 5% to 15%. Furthermore, the permeability is reduced by approximately 97% upon the addition of CW and a tiny quantity of OPC. These findings support the beneficial effects of CW and OPC on the soil; these novel compounds may find application as road layer stabilizers. By connecting between soil particles, CW fine particles—a mineral component of CW and OPC reduced the spaces.

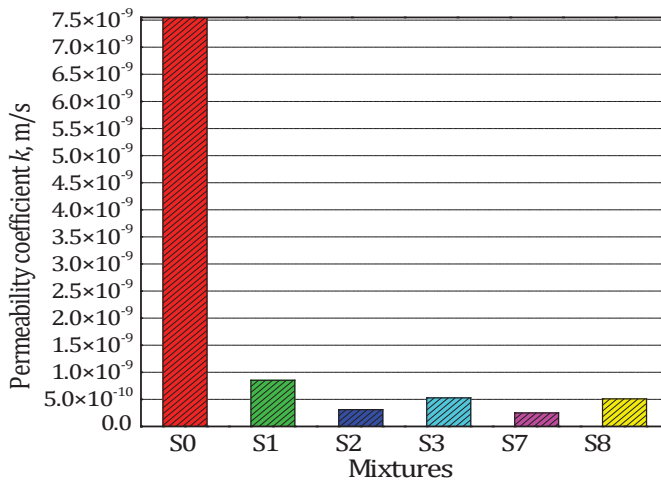


Figure 6. Effect of CW, OPC on permeability of stabilised soils

2.3. UCS test

UCS is an important test for soil improvement as reported by Sariosseiri & Balasingam (2013). UCS tests were performed in this inquiry to look at the effects of CW ration, CW with OPC dosage, and curing conditions on stabilised soil. The investigation and discussion of every specimen are provided in Sections 2.1.1.–2.1.4.

2.3.1. Influence of CW on UCS of stabilised soil

Soil troubles are seen in Figure 7, where it is noticed that the UCS decreases from 748 KPa in an unsullied state to 0 KPa in an immersed state. Soil particle separation and cohesiveness degradation occur when the specimens are submerged in water, a condition that might cause issues for the sub-base layer of newly constructed roads.

The UCS rises when the amount of CW in the soil is increased from 5% to 10% when it is not saturated. In addition to adding 15% CW to the soil, the UCS decrease a bit compared to dosage of 5 and 10%. Positive CW effect filled the spaces between soil particles in the soil. However, the CW reach of silica (SiO_2) and the soil reach of CaO may have triggered interactions between these two important minerals. Combinations of SiO_2 with CaO result in calcium silicate, which many researchers employ to stabilise soil by making it more compressively strong.

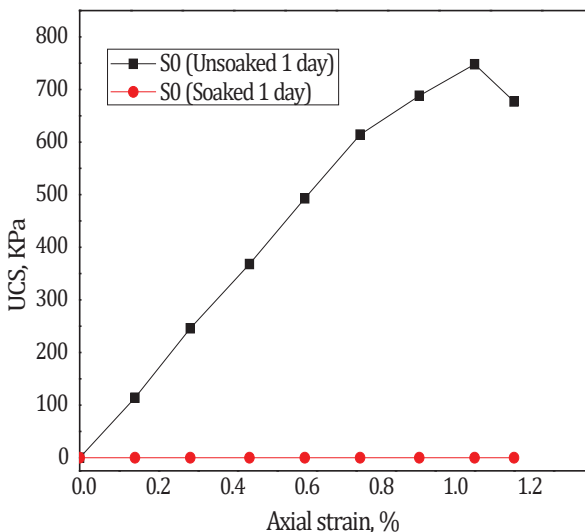


Figure 7. UCS Values of natural soil

As the CW grew from 5% to 15%, as seen in Figure 8, the UCS increased by almost 23%. The dosages of CW at 5%, 10%, and 15% on UCS are shown in Figure 9, with 922 KPa being the ideal UCS. The UCS of stabilised soils is significantly impacted by waste ceramic dust, as noted by Chen & Indusuyi (2015). According to Cabalar et al. (2016), UCS was impacted when CW tile was used for subgrade materials.

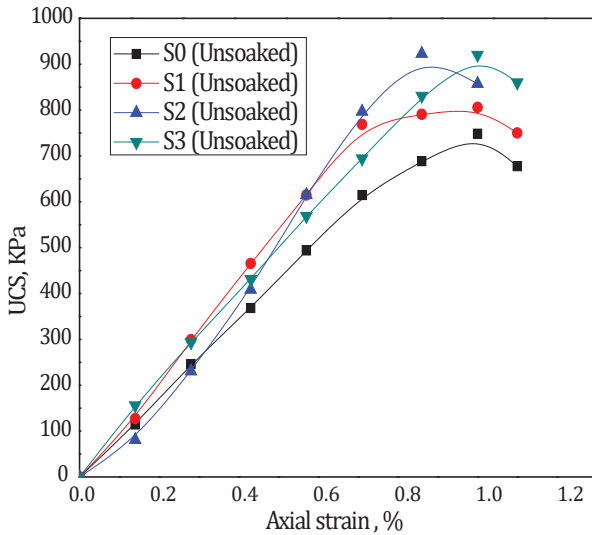


Figure 8. Effect of CW on UCS results of soil with 5, 10 and 15% CW

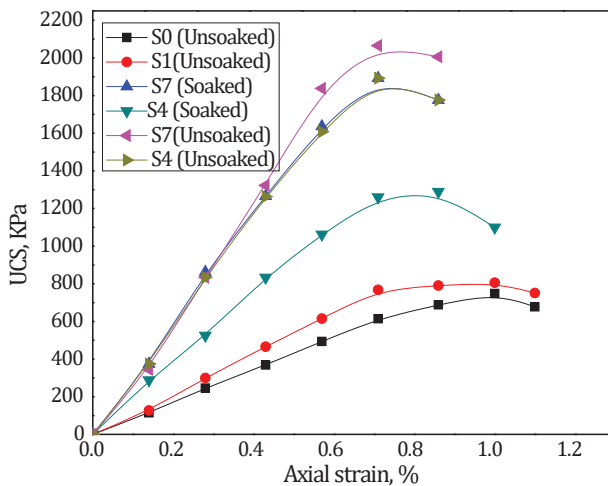


Figure 9. Influence of 5 % CW and 1.5 to 2% OPC on UCS of stabilised soils

2.3.2. Influence of CW and OPC on UCS of stabilised soil

Figure 10 shows that adding 1.5–2% OPC and 5% CW raises the stabilised soil UCS from around 72.3% to 176% when it is unsoaked and to 2 MPa when it is soaked. Furthermore, because OPC and CW have large percentages of alumina, silica, and silica in their mineral compositions, respectively, CW and cement also develop novel stiff materials.

Additionally, we can see from Figure 11 that when 10% CW was added, the OPC ranged between 1.5 and 2% and the UCS increased approximately from 92% to 152% and 118% to 137% in both conditions (soaked and unsoaked), respectively. The results of UCS as observed in mixtures with 5% CW are maintained when CW is increased from 5% to 15%.

On the other hand, UCS increased by 106% to 137% in combinations with 15% CW and 1.5% to 2% OPC, as seen in Figure 12. The good UCS outcome was affected by the inclusion of CW and a tiny quantity of OPC. However, CW and OPC have different compositions, natural soil properties set them apart and create a distinct matrix.

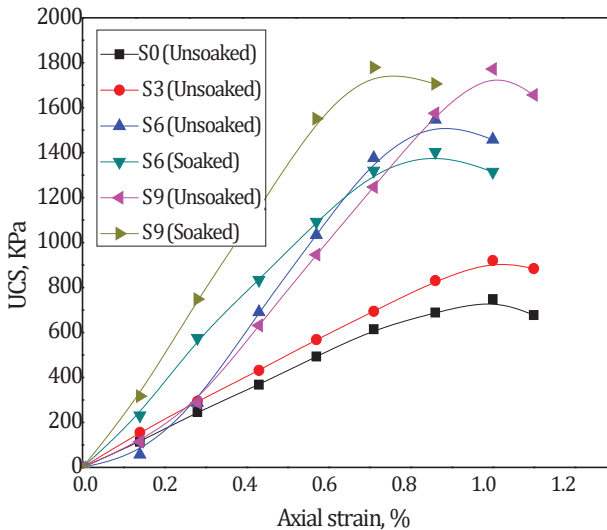


Figure 10. Influence of 10 % CW and 1.5 to 2% OPC on UCS of stabilised soils

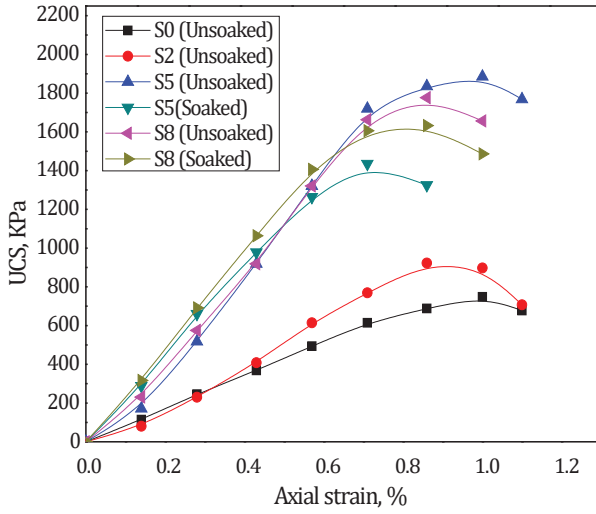


Figure 11. Influence of 15 % CW and 1.5 to 2% OPC on UCS of stabilised soils

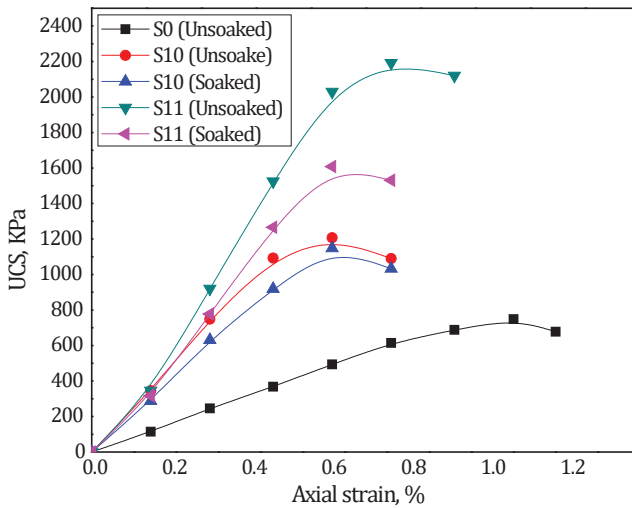


Figure 12. Influence of 1.5 to 2% OPC on UCS of stabilised soils

2.3.3. Influence of CW and OPC on UCS of stabilised soil

Figure 13 shows the outcomes of the UCS test conducted on treated soil containing various amounts of CW. It was found that until the UCS reached 2 MPa, the UCS rose as the OPC ratio increased. It is verified that the combination of CW and OPC composition provides hard materials appropriate for usage as sub-base layers in road building. However, samples with 5, 10, and 15% CW with 2% OPC as a partial stabiliser replacement and a higher UCS of 2.1 MPa are shown in Figure 14.

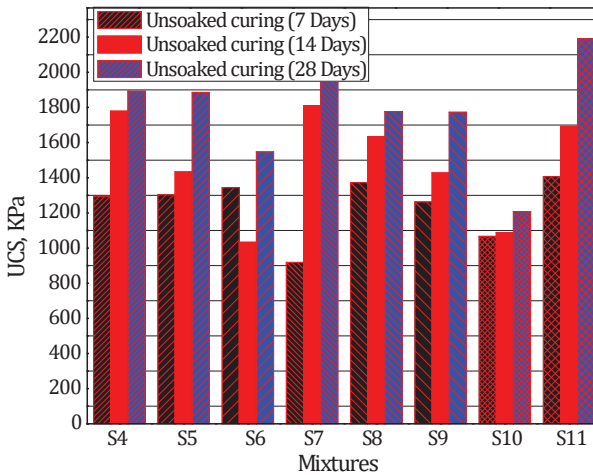


Figure 13. Influence of unsoaked curing on UCS of stabilised soils

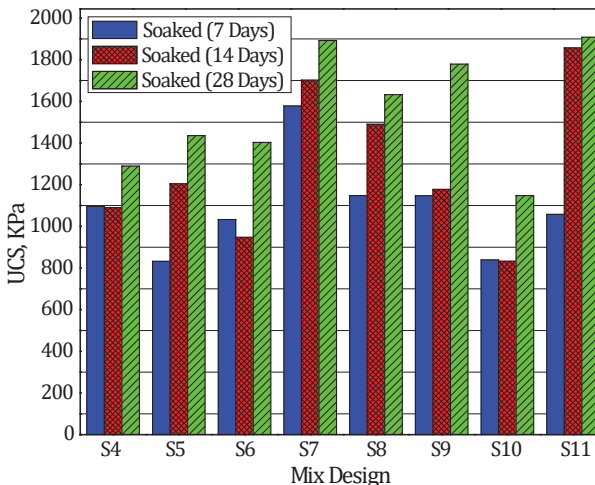


Figure 14. Influence of soaked curing on UCS of stabilised soils

2.3.4. Influence of curing time and conditions on UCS of stabilised soil

The UCS of stabilised soils rose with increasing curing time, as demonstrated by Figures 15 and 16. This indicates that the OPC and CW act when combined with soil that has stabilisers and water. Hard mass was created by the pazzolanic reaction, which decreased the voids in the newly formed matrix. Longer curing times equilibrate the ultimate strength (Chand & Subbarao, 2007).

Yeo (2008) states that for medium- to high-volume roads, the minimum UCS needed for the sub-base layer is 2 MPa, and for low-volume roads, it is 12 MPa. However, Syed & Scullion (2001) stated that 1.38 MPa is the minimum UCS needed for medium-to high-volume highways. IRC:37 (2012) states that 750 KPa is the minimum UCS of stabilised samples for the sub-base layer of low-volume roads after 28 days of curing. The majority of our combinations achieved the minimum UCS values needed, which leads us to the conclusion that stabilizing soil containing CW and a small quantity of cement are appropriate materials for the road sub-base layer.

The links between permeability and CBR, as shown in Figure 17, support the idea that adding CW and OPC to the soil improves it. It is evident that raising CBR decreases permeability. OPC binds between CW and soil, creating a stiff substance, while CW fills the spaces between soil

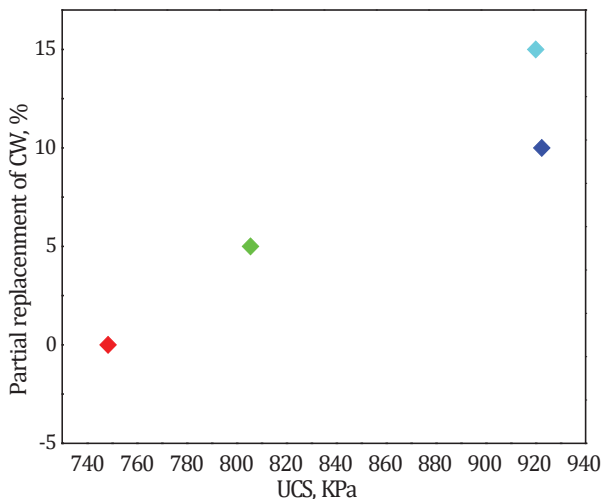


Figure 15. Effect of the CW replacement on the UCS of stabilised soil specimen

particles. From Figure 17, we can conclude that the optimum ratio of CW to the soil should be less than 15% because adding 15% CW without cement to the soil decreased the results of CBR and increased the permeability.

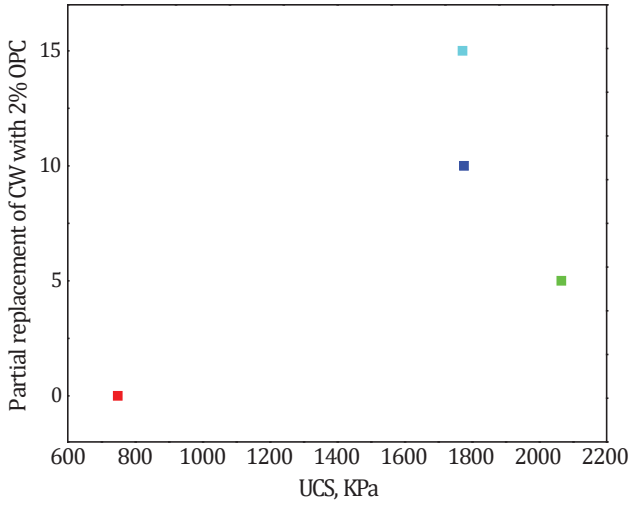


Figure 16. Effect of the CW and OPC of partial replacement on the UCS of stabilised soil specimens

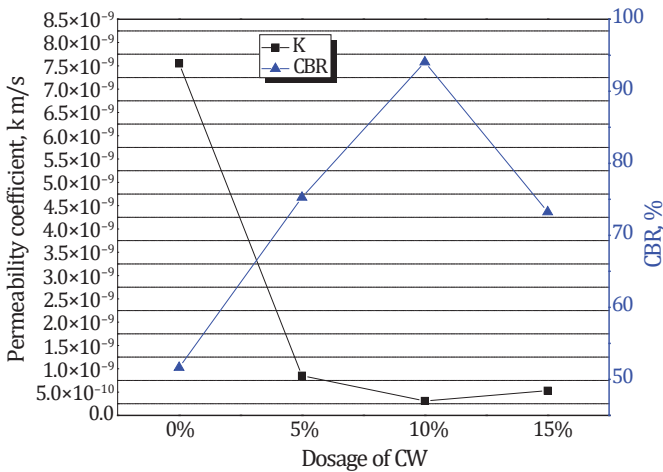


Figure 17. Relationship between permeability and CBR

2.4. Influence of CW on the consolidation of soil

Figures 18 and 19 illustrate the consolidation results on unstabilised and stabilised soil with varying amounts of CW and OPC. Figure 18 illustrates how raising CW from 5% to 15% results in a decrease in the void ratio. On the other hand, Figure 19 shows how the compression index drops by approximately 61.7% and 31.7%, respectively, when CW 5%, 10%, and 15% are added. Reduction C_c suggests that there may have been improvements in the CW-treated soil. According to Pastor et al. (2019), adding 25% limestone powder to soil reduces its compression index by 27%.

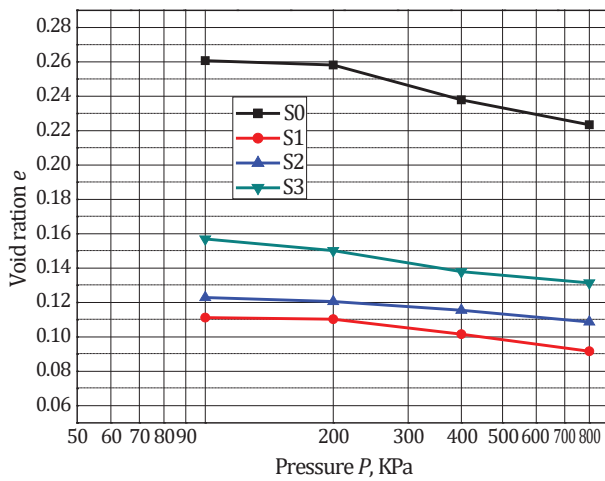


Figure 18. e-log P curve for different mixtures

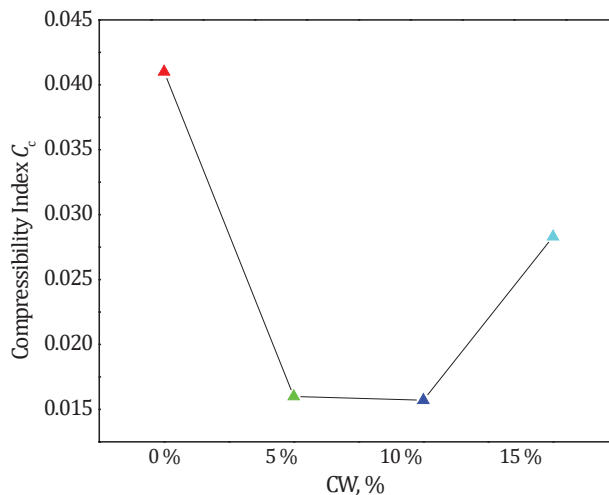


Figure 19. Variation of compression index (C_c) with CW

2.5. Influence of CW and OPC on microstructure of CW-OPC stabilised soil

The SEM images of the untreated soil (S0), treated soil (S7), treated soil (S8), and stabilised soil (S9) with 5% CW and 2% OPC are shown in Figure 20. This last photo shows the treated soil with 10% CW and 2% OPC. The large pores seen in Figure 20(a) attest to the inferior mechanical properties of CBR and UCS. When 5% and 10% CW and 2% OPC are added to the soil, the microstructure of the soil significantly changes, as seen in Figures 20(b) and 20(c). This shows that a new stiff

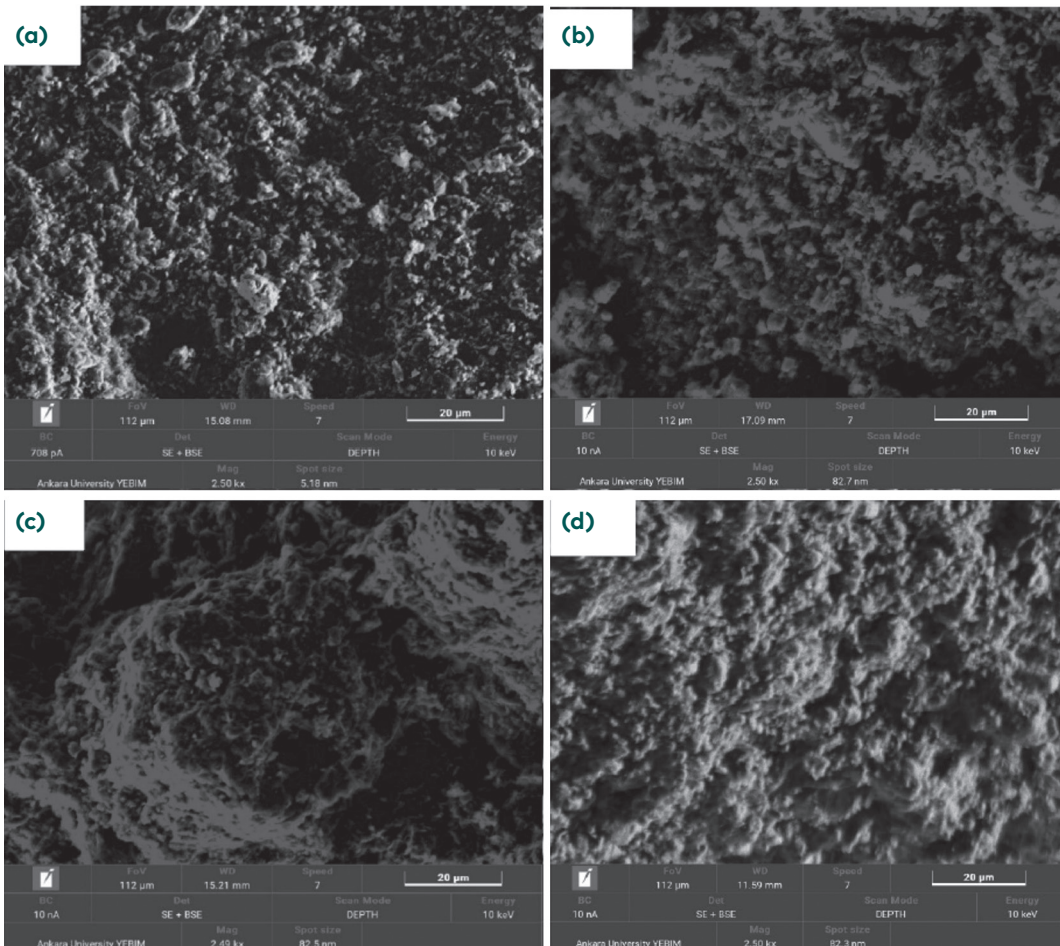
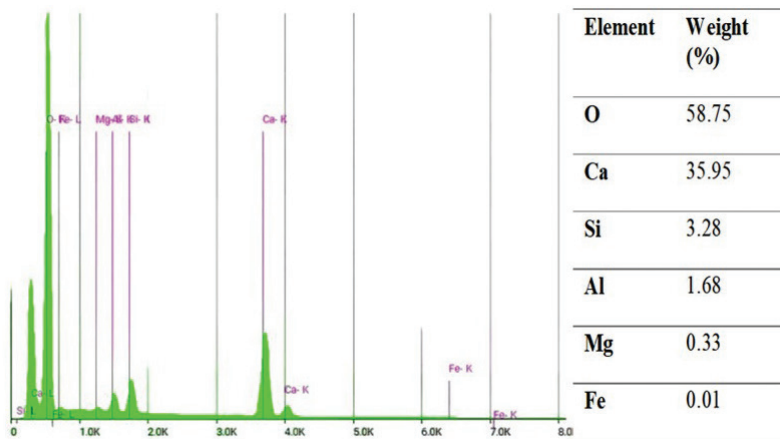


Figure 20. (a) SEM of S0 (Magnitude 2500×); (b) SEM of S7 (Magnitude 2500×); (c) SEM of S8 (Magnitude 2500×); (d) SEM of S9 (Magnitude 2500×)

matrix is formed when the CW and OPC bind between the soil particles. When 5% and 10% CW are added with 2% OPC, an advanced pozzolanic reaction occurs. On the other hand, Figure 20(d) shows that adding 15% CW and 2% OPC results in larger pores, suggesting that 10% of the mixture total weight is the ideal amount of CW. Comparable results were observed by Arrigoni et al. (2017) when fly ash (FA) and cement were applied to the soil. Furthermore, James & Pandian (2018) research shows that adding micro-ceramic dust to the soil in addition to lime has a similar impact on microstructural features.

(a) EDS spectra for natural soil



(b) EDS spectra for stabilised soil

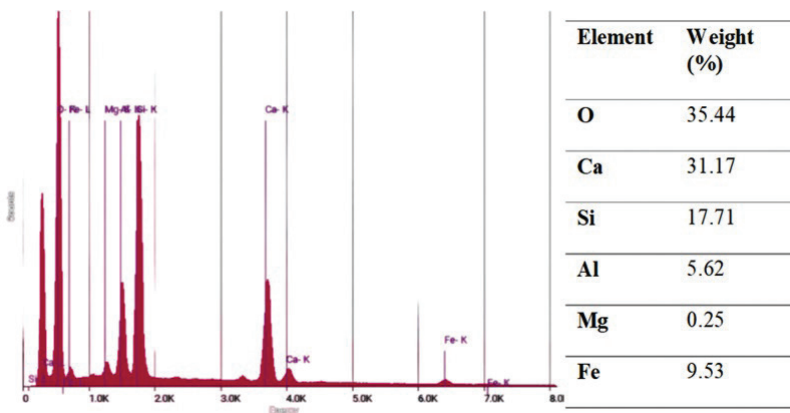


Figure 21. EDS spectra for natural soil and stabilised soil

The EDS analysis of the chemical components of untreated and treated soil with CW and OPC is displayed in Figures 21(a) and 21(b). The treated samples show the presence of the new elements Si, Ca, and Al, which are in charge of the calcium-aluminum-silicate hydrates (S-A-S-H) production. As a result, according to Al-Bared et al. (2018), CW and OPC can cooperate chemically with the soil particles in 2.6 Infrared spectroscopy.

Figure 22 shows IR spectroscopy of untreated and treated soil with 5%, 10%, and 15% of CW and 5% CW+2% OPC. Figure 22, which displays independently observed absorption bands, shows the mutual features found in the infrared spectra of soil that has been stabilised and that has not. The IR spectra of soil and CW are dominated by Si-O-Al and Si-O-Si bands in the representative absorption band observed in the range of 1035 cm^{-1} to 874 cm^{-1} . This indicates that the incorporation of these materials with CW and OPC will convert cementitious when water is added to the new matrix due to the consistency of (C-S-H) and (C-A-H) (Moraes et al., 2019).

The band forming for the vertical and in-plane Si-O stretching is ascribed to the Ca-OH band, which occurs due to stabilised soil with CW and CW+OPC, respectively. Additionally, when CW to the soil increased, Figure 22 demonstrates that the intensity of particular wavelengths

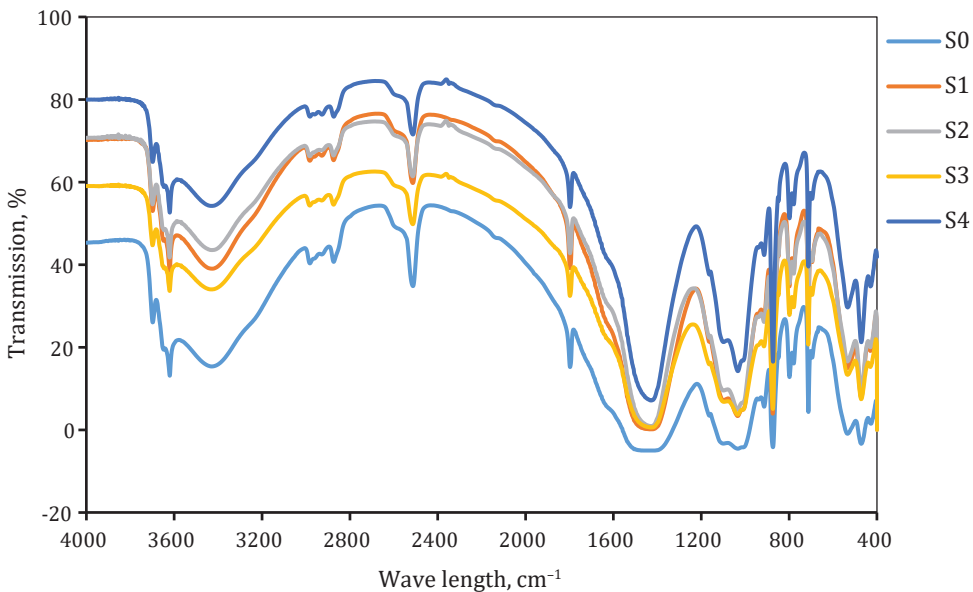


Figure 22. FTIR spectrums for untreated and treated soil with CW and CW with OPC

decreased, as seen by the reduction of relative points presented in the 533 cm^{-1} to 471 cm^{-1} range. Lemouagna et al. (2014) and Wi et al. (2018) found that OH stretching vibrations matching inner-surface hydroxyls could be attributed to additional peaks at 3620 cm^{-1} and 3698 cm^{-1} . These results yielded similar outcomes with different researchers. The stretching vibration at 3425 cm^{-1} is the source of the remaining bands.

2.7. Mercury intrusion porosimetry tests

An extensive screening of the MIP results for different ranges of pores was done in order to determine the impact of CW and OPC on porosity distribution. The treated soil pore size distribution as determined by the MIP test is displayed in Figure 23. The pore size distribution of several stabilised soil combinations is shown in Figure 23. Furthermore, according to Figure 23, the essential pore size of natural soil was between 0.1 and $1\text{ }\mu\text{m}$; however, the stabilised mixtures shifted to the right side, which resulted in a decrease in pore size. The addition of CW from 5 to 15% and CW with 2% OPC lowered the pore size. The outcomes of the UCS, permeability, and consolidation tests are supported by these findings. Aldaood et al. (2014) revealed similar observations about the effects of lime-stabilised gypseous soils.

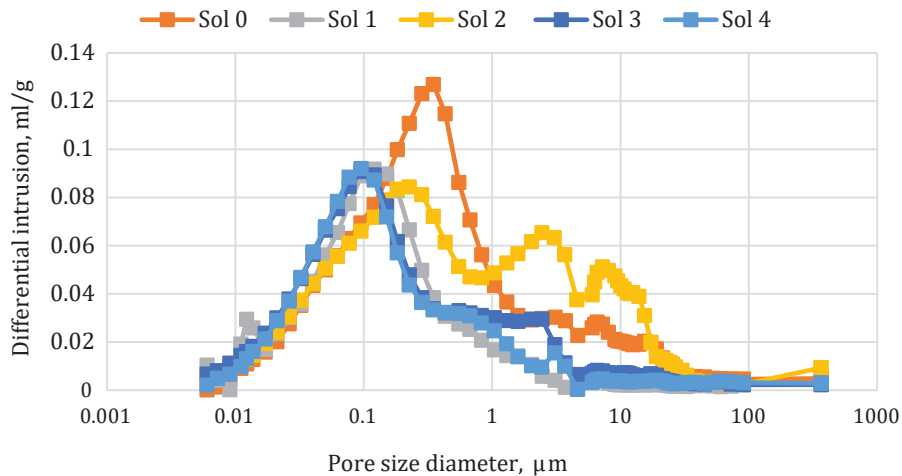


Figure 23. Changes in pore size distribution of untreated and treated soil

Conclusion

The goal of the experimental study is to determine how permeability, UCS, and consolidation behaviour may be impacted by CW and CW-OPC. A series of experiments determined the mechanical and hydraulic properties, and microstructures of treated and untreated soils, as well as a Guelph permeameter to validate the problematic nature of our project. The results and specifics of the present study are as follows:

- Due to its high in-situ permeability, natural soil is highly susceptible to water.
- The permeability of the soil treated with CW and cement was reduced by approximately 97%, indicating that CW had a beneficial effect by filling in the spaces between soil particles. On the other hand, the OPC mixes support the pozzolanic reaction by generating hard materials.
- The soil-CW cement showed greater UCS values in both conditions, which went above 2 MPa; nevertheless, the UCS of soil-CW increased with increasing CW in wet conditions and losses in immersed conditions.
- When the percentage of CW rose from 5% to 10%, the compression index dropped by around 67%. This work demonstrates the beneficial interactions between CW and OPC, which may lead to the development of novel substitute materials for road sub-base layers.
- Microscopic examination supported the mechanical and hydraulic results by showing that the CW and OPC improve soil properties by lowering waves and pore size in stabilised materials.
- Using CW and OPC together offers a practical way to enhance the qualities of road sub-base layers.

Acknowledgements

The University Mohamed El Bachir El Ibrahimi of Bordj Bou Arreridj financially supported the research described in this work under grant (No. A01L02UN340120230004), and we thank GEO-LAB for supporting this project through experimental tests.

Funding

This work was supported by the University Mohamed El Bachir El Ibrahimi of Bordj Bou Arreridj under Grant (No. A01L02UN340120230004).

REFERENCES

- Arrigoni, A., Pelosato, R., Dotelli, G., Beckett, C. T. S., & Ciancio, D. (2017). Weathering's beneficial effect on waste-stabilised rammed earth: a chemical and microstructural investigation. *Construction and Building Materials*, *140*, 157–166. <https://doi.org/10.1016/j.conbuildmat.2017.02.009>
- Arulrajah, A., Piratheepan, J., Disfani, M. M., & Bo, M.W. (2012). Resilient moduli response of recycled construction and demolition materials in pavement subbase applications. *Journal of Materials in Civil Engineering*, *25*(12), 1920–1928. [https://doi.org/10.1061/\(ASCE\)MT.1943-5533.0000766](https://doi.org/10.1061/(ASCE)MT.1943-5533.0000766)
- Ahmed, A. A., & Abouzeid, A. Z. M. (2009). Potential use of phosphate wastes as aggregates in road construction. *Journal of Engineering Sciences*, *37*(2), 413–422. <https://doi.org/10.21608/jesaun.2009.125357>
- Aldaood, A. M., Bouasker, M., & Al-Mukhtar, M. (2014). Free swell potential of lime-treated gypseous soil. *Applied Clay Science*, *102*, 93–103. <https://doi.org/10.1016/j.clay.2014.10.015>
- Al-Bared, M. A. M., Marto, A., & Latifi, N. (2018). Utilization of recycled tiles and tyres in stabilization of soils and production of construction materials-A: State-of-the-art review. *Korean Journal of Civil Engineering*, *22*, 3860–3874. <https://doi.org/10.1007/s12205-018-1532-2>
- ASTM D 5126. (2016). Standard guide for comparison of field methods for determining hydraulic conductivity in Vadose Zone. US. <https://www.astm.org/d5126-16e01.html>
- ASTM D5084-10. (2010). Standard test methods for measurement of hydraulic conductivity of saturated porous materials using a flexible wall permeameter. US. <https://www.astm.org/d5084-00.html>
- ASTM 2166-06. (2006). Standard test method for unconfined compressive strength of cohesive soil. US. <https://cdn.standards.iteh.ai/samples/51097/96d2e1c56e544f8ba9810747b9d2a032/ASTM-D2166-06.pdf>
- ASTM D2435. (2011). Standard test methods for one-dimensional consolidation properties of soils using incremental loading, standard. US. <https://www.astm.org/d2435-04.html>
- Cabalar, A. F., Hassan, D. I., & Abdulnaffaa, M. D. (2016). Use of waste of ceramic tile for road pavement subgrade. *Road Materials and Pavement Design*, *18*(4), 882–896. <https://doi.org/10.1080/14680629.2016.1194884>
- Chand, S. K., & Subbarao, C. (2007). Strength and slake durability of lime stabilized pond ash. *Journal of Materials in Civil Engineering*, *19*(7), 601–608. [https://doi.org/10.1061/\(asce\)0899-1561\(2007\)19:7\(601\)](https://doi.org/10.1061/(asce)0899-1561(2007)19:7(601))
- Chen, J. A., & Idusuyi, F. O. (2015). Effect of waste ceramic dust (WCD) on index and engineering properties of shrink-swell soils. *International Journal of Engineering and Modern Technology*, *1*(8), 52–62.
- Daniyal, M. D., & Shakeel, A. (2015). Application of waste ceramic tile aggregates in concrete. *International Journal of Innovative Research in Science, Engineering and Technology*, *4* (12), 12808–12815. https://www.ijirset.com/upload/2015/december/128_32_Application.pdf

- Darcy, H. (1856). Les fontaines publiques de la ville de Dijon: exposition et application des 753 principes à suivre et des formules à employer dans les questions de distribution d'eau. Victor 754 Dalmont, Paris.
- Edeboucha, S., Mamoune, S. M. A., Sail, Y., & Ziani, H. (2020). Effects of ceramic waste, marble dust, and cement in pavement sub-base layer. *Geotechnical and Geological Engineering*, 38(3), 3331–3340. <https://doi.org/10.1007/s10706-020-01211-x>
- Electricwala, F., Ankit, J., & Rakesh, K. (2013). Ceramic dust as construction material in rigid pavement. *American Journal of Civil Engineering and Architecture*, 1(5), 112116. <https://doi.org/10.12691/ajcea-1-5-5>
- Gautam, P. K., Kalla, P., Jethoo, A. S., Agrawal, R., & Singh, H. (2018). Sustainable use of waste in flexible pavement: A review. *Construction and Building Materials*, 180, 239–253. <https://doi.org/10.1016/j.conbuildmat.2018.04.067>
- Gnanendran, C. T., & Dalim, K. P. (2016). Fatigue characterization of lightly cementitiously stabilised granular base materials using flexural testing. *Journal of Materials in Civil Engineering*, 28 (9). [https://doi.org/10.1061/\(ASCE\)MT.1943-5533.0001598](https://doi.org/10.1061/(ASCE)MT.1943-5533.0001598)
- Head, K. H. (1982). Manual of soil laboratory testing. Permeability shear strength and compressibility tests (2nd ed.) London, Penteh Press.
- IRC:37. (2012). Tentative guidelines for the design of flexible pavements. New Delhi, India. <https://law.resource.org/pub/in/bis/irc/irc.gov.in.037.2012.pdf>
- James, J., & Pandian, P. K. (2018). Strength and microstructure of micro ceramic dust admixed lime stabilized soil. *Journal of Construction*, 17(1), 5–22. <https://doi.org/10.7764/RDLC.17.1.5>
- Jafari, M., & Esna-asari M. (2012). Effect of waste tire cord reinforcement on unconfined compressive strength of lime stabilised clayey soil under freeze-thaw condition. *Cold Regions Science and Technology*, 82, 21–29. <https://doi.org/10.1016/j.coldregions.2012.05.012>
- Koyuncu, H., Guney, Y., Yilmaz, G., Koyuncu, S., & Bakis, R. (2004). Utilization of Ceramic Wastes in the Construction Sector. *Key Engineering Materials*, 264–268, 2509–2512. <https://doi.org/10.4028/www.scientific.net/kem.264-268.2509>
- Lemougna, P. N., Madi, A. B., Kamseu, E., Melo, U. C., Delplancke, M. P., & Rahier, H. (2014). Influence of the processing temperature on the compressive strength of Na activated lateritic soil for building applications. *Construction and Building Materials*, 65, 60–66. <https://doi.org/10.1016/j.conbuildmat.2014.04.100>
- Moraes, M. J. B., Moraes, J. C. B., Tashima, M. M., Akasaki, J. L., Soriano, L., Borrachero, M. V., & Payá, J. (2019). Production of bamboo leaf ash by auto-combustion for pozzolanic and sustainable use in cementitious Matrices. *Construction and Building Materials*, 208, 369–380. <https://doi.org/10.1016/j.conbuildmat.2019.03.007>
- Ojuri, O. O., & Opeyemi, E. O. (2014). Strength characteristics of lead and hydrocarbon contaminated lateritic soils stabilised with lime-rice husk ash. *Electronic Journal of Geotechnical Engineering*, 19(Z2), 10027–10042. https://eprints.lmu.edu.ng/1680/1/Strength_Characteristics_of_Lead_and_Hyd.pdf

- Onakunle, O., Omole, D. O., & Ogbyie, A. S. (2019). Stabilization of lateritic soil from Agbara Nigeria with ceramic waste dust. *Cogent Engineering*, 6(1), Article 1710087. <https://doi.org/10.1080/23311916.2019.1710087>
- Pastor, J. L., Tomás, R., Cano, M., Riquelme, A., & Gutiérrez, E. (2019). Evaluation of the improvement effect of limestone powder waste in the stabilisation of swelling clayey soil. *Sustainability*, 11(3) 679. <https://doi.org/10.3390/su11030679>
- Rajamannan, B., Viruthagiri, G., & Suresh Jawahar, K. (2013). Effect of grog addition on the technological properties of ceramic brick. *International Journal of Latest Research in Science and Technology*, 2(6), 81–84. https://www.mnkjournals.com/journal/ijlrst/pdf/Volume_2_6_2013/10234.pdf
- Reynolds, W. D., & Elrick, D. E. (1986). A method for simultaneous in situ measurement in the Vadose Zone of field-saturated hydraulic conductivity, sorptivity and the conductivity-pressure head relationship. *Ground Water Monitoring and Remediation*, 6(1), 84–85. <https://doi.org/10.1111/j.1745-6592.1986.tb01229.x>
- Sariosseiri, F., & Muhunthan, B. (2013). Effect of cement treatment on geotechnical properties of some Washington state soils. *Engineering Geology*, 104(12), 119125. <https://doi.org/10.1016/j.enggeo.2008.09.003>
- Syed, I. M., & Scullion, T. (2001). Performance evaluation of recycled and stabilised bases in Texas. *Transportation Research Record*, 1757(1), 14–21. <https://doi.org/10.3141/1757-02>
- Valdés, A. J., Martínez, C. M., Romero, M. G., García, B. L., Del Pozo, J. M., & Vegas, A. T. (2010). Re-use of construction and demolition residues and industrial wastes for the elaboration or recycled eco-efficient concretes. *Spanish Journal of Agricultural Research*, 8(1), 25–34. <https://doi.org/10.5424/sjar/2010081-1140>
- Wi, K., Lee, H. S., Lim, S., Song, H., Hussin, M. W., & Ismail, M. A. (2018). Use of an agricultural by-product, nano sized palm oil fuel ash as a supplementary cementitious material. *Construction and Building Materials*, 183, 139–149. <https://doi.org/10.1016/j.conbuildmat.2018.06.156>
- Xuan, D. X., Molenaar, A. A. A., & Houben, L. J. M. (2016). Shrinkage cracking of cement treated demolition waste as a road base. *Materials and Structures*, 49, 631–640. <https://doi.org/10.1617/s11527-015-0524-7>
- Yeo, R. (2008). The development and evaluation of protocols for the laboratory characterisation of cemented materials. Sydney: Austroads.
- Zhang, Z. F., Groenveld, P. H., & Parkin, G. W. (1998). The well shape-factor for the measurement of soil hydraulic properties using the Guelph Permeameter. *Soil and Tillage Research*, 49(3), 219221. [https://doi.org/10.1016/S0167-1987\(98\)00174-3](https://doi.org/10.1016/S0167-1987(98)00174-3)